# A stress relaxation strategy for preparing high-quality organic-inorganic perovskite thin films via vapor-solid reaction

*Shenghan Hu[a], Changyu Duan[a], Hongqiang Du[a], Shuang Zeng[a], Anqi Kong[a], Yuanyuan Chen[a], Yong Peng[a], Yi-Bing Cheng[a,b] and Zhiliang Ku[*a]*

[a]State Key Lab of Advanced Technologies for Materials Synthesis and Processing, Wuhan University of Technology, 122 Luoshi Road, Wuhan 430070, Hubei Province, China

[b]Foshan Xianhu Laboratory of the Advanced Energy Science and Technology Guangdong Laboratory, Foshan 528216, Guangdong Province, China

* Corresponding author: Zhiliang Ku, E-mail: zhiliang.ku@whut.edu.cn
Keywords: Stress relaxation; thin film; Vapor-solid reaction; Perovskite; Solar cell

**Materials:**

All the reagents and chemicals were used as received without further treatment. Formamidinium iodide (FAI,99%), Formamidinium Chloride (FACl,99%) were purchased from Suzhou Xurou Optoelectronics Technology Corp). Methylammonium iodide (MAI,99%), Propylammonium Iodide (PAI,99%), Butylamine iodide (BAI,99%), Hexaneammonium iodide (HAI,99%) Cesium bromide (CsBr,99%), lead iodide ($PbI_2$,99.99%), Li-TFSI, FK209, 4-tert-butylpyridine (TBP) and PCBM were purchased from Xi'an Polymer Light Technology Corp. Anhydrous ethanol (99.7%) and Tin (II) chloride dihydrate ($SnCl_2 \cdot 2H_2O$) was purchased from Sigma-Aldrich. Other materials were purchased from Shanghai Aladdin Biochemical Technology Co. and Sinopharm Chemical Reagent Co. LTD used as received.

**Device fabrication**

Preparation of FTO/$SnO_x$ substrates:

The etched FTO glass was placed in a cleaning container and sonicated with detergent, deionized water, and anhydrous ethanol for 15 minutes in sequence. The $SnO_x$ precursor was prepared by mixing1.096g of $SnCl_2 \cdot 2H_2O$, 5g of urea,5mL of hydrochloric acid,100μL of thioglycolic acid per 400mL of deionized water, then stored in a refrigerator below 5℃ for use. The FTO/$SnO_x$ substrates were prepared by chemical bath deposition (CBD) approach as follows: firstly, immerse the pre-cleaned

FTO glass in a $SnO_x$ precursor solution for 3h at 90 °C; secondly, FTO/ $SnO_x$ substrates were sonicated with deionized water for about five minutes and flushed with deionized water three times, then dried quickly by an air gun. Finally, the dried FTO/ $SnO_2$ substrates are annealed on a 170℃ hot plate for one hour.

**Preparation of perovskite films**

Deposition of CsBr/$PbI_2$ composite precursor film: CsBr (around 0.3-0.5 Å/s rate, 30 nm) and $PbI_2$ (around 3-5 Å/s rate, 300 nm) were depositions through thermal evaporation on the FTO/$SnO_x$ substrates under $8\times10^{-6}$ bar without annealing substrates.

Preparation of organic vapor source: FAI/FACl hybrid vapor source were deposited on glass substrates by ultrasonic spraying 20 mL FAI ethanol solution containing 500 mg FAI and 50 mg FACl.

Solid-vapor reaction: the composite precursor film and organic vapor source were placed in a self-designed vacuum chamber with (170 ℃, 30 Pa) for a three minutes solid-vapor reaction to form control perovskite films. Then perovskite films which need annealing were put in a chamber at the corresponding temperature of the atmospheric environment for 15 minutes. Perovskite films which need vapor annealing were put in the same chamber at the 170 ℃ of the atmospheric environment and passed into the corresponding organic vapor.

The sample status explanation appealing in article. **Control sample:** perovskite film after three minutes of solid-vapor reaction. **Annealing sample:** perovskite film after three minutes of solid-vapor reaction and then annealed at 170 ℃ on a hot plate. **Vapor-annealing sample:** perovskite film after three minutes of solid-vapor reaction and then annealed 170 ℃ of the atmospheric environment and passed into the PAI vapor.

**Preparation of Spiro-OMeTAD films and Au electrode**

The Spiro-OMeTAD solution was prepared by dissolving 91.4 mg Spiro-OMeTAD into 1 mL chlorobenzene followed by the adding 18 μL Li-TFSI (pre-dissolved as a 520 mg/mL stock solution in acetonitrile), 11.4 μL FK209 (pre-dissolved

as a 300 mg/mL stock solution in acetonitrile) and 35.5 μL 4-tert-butylpyridine in the solution. Spiro-OMeTAD films were deposited by spin-coating at 4000 rpm for 20 s in $N_2$-filled glovebox. Finally, 80 nm thick gold was thermally evaporated on top of the Spiro-OMeTAD films as the back contact. In the end, an Au electrode (80 nm) was thermally evaporated onto the Spiro-OMeTAD film under a pressure of $6\times10^{-4}$ Pa.

**Characterization**

The surface morphologies were investigated by scanning electron microscopy (SEM S-4800, Hitachi) with an accelerating voltage of 5 kV. Atomic Force Microscopy

(AFM) topography images were acquired on ( Asylum Research, Oxford Instruments ). The X-ray diffraction (XRD) patterns of the samples and residual stress test were recorded using an X-ray diffractometer (XRD, D8 Advance) and analyzed by jade 6.5 software. The grazing incidence X-ray diffraction (GIXRD) measurements were characterized using a PANalytical Empyrean diffractometer. Grazingincidence wide-angle X-ray scattering (GIWAXS) was obtained by (Dectris EIGER2 Si 1M). The UV−vis absorption spectra were measured by a UV−vis spectrometer (Lambda 750S, PerkinElmer). The photoluminescence (PL) and time-resolved photoluminescence (TRPL) spectra were obtained from Delta Flex Flux Fluorescence Lifetime System (HORIBA Scientific Company, Japan). The fluorescence lifetime imaging (FLIM) was observed by Time-resolved fluorescence confocal microscopy and spectral testing system (PicoQuant Micro Time100). The chemical compositions of the samples were carried out using X-ray photoelectron spectroscopy (XPS) (EscaLab Xi+, Thermo Scientific) equipped with a monochromatic Al Kα X-ray source (hν = 1486.6 eV). TAS was performed with a HELIOS femtosecond transient absorption (Ultrafast System, LLC). The 400 nm pump pluses were generated by a 1 kHz, 85 fs Ti: sapphire ultrafast laser amplifier under pump power of 2μW. The photocurrent density-voltage (J-V) characteristics of solar cells were measured under AM 1.5G illumination at 100 $mW/cm^2$ (Oriel 94023A, 300 W) and a Keithley 2400 source meter. All the devices

were tested under AM 1.5G sunlight (100mW $cm^{-2}$) using a metal mask of 0.1475 $cm^2$ with a scan rate of 10 mV/s. Quasi-stabilized power output (q-SPO) was recorded for 120 s at the potential corresponding to the maximum power point in the reverse J-V curve. The external quantum efficiency (EQE) was measured by an EQE system (in Newport, USA PT-QEM1000) which has been calibrated by Newport and EQE data was measured from 280 nm to 850 nm with an interval of 10 nm. Space charge limited current (SCLC), Electrical impedance spectroscopy (EIS) and Mott-Schottky analyses were measured by a Chenhua electrochemistry workstation under dark conditions.

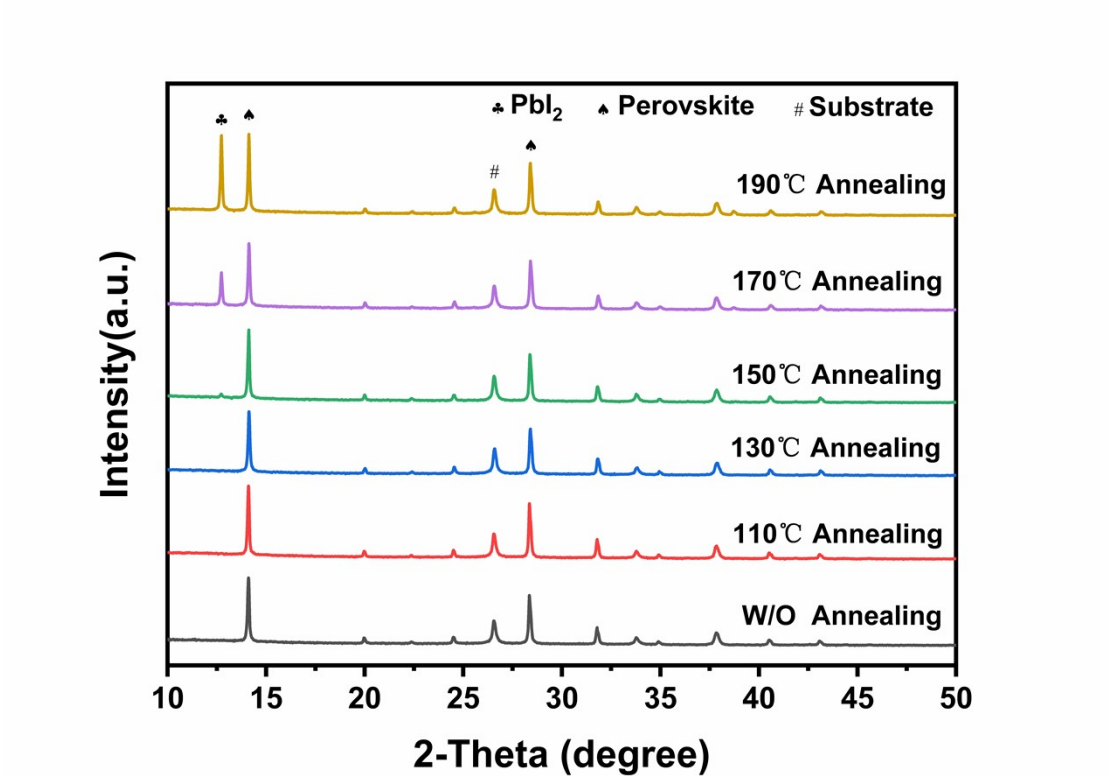


**Figure S1**. XRD patterns of the perovskite thin films with different annealing temperatures.

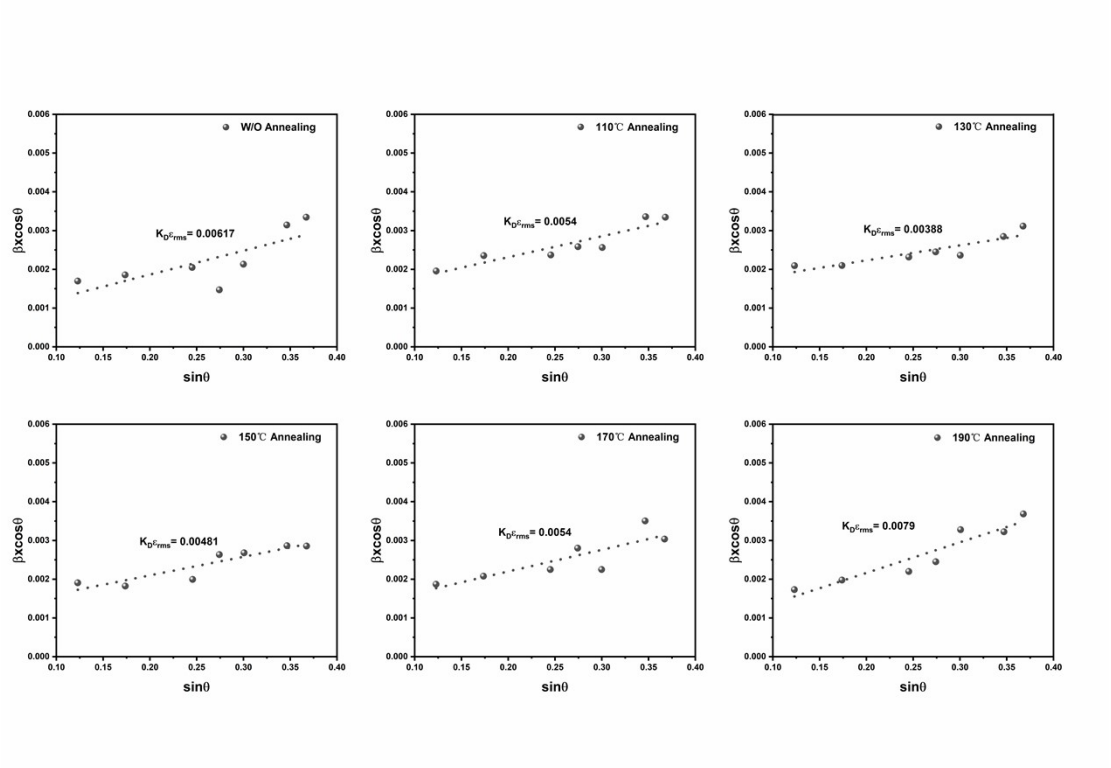


**Figure S2**. Williamson−Hall plots of perovskite films W/O and with different annealing temperatures.

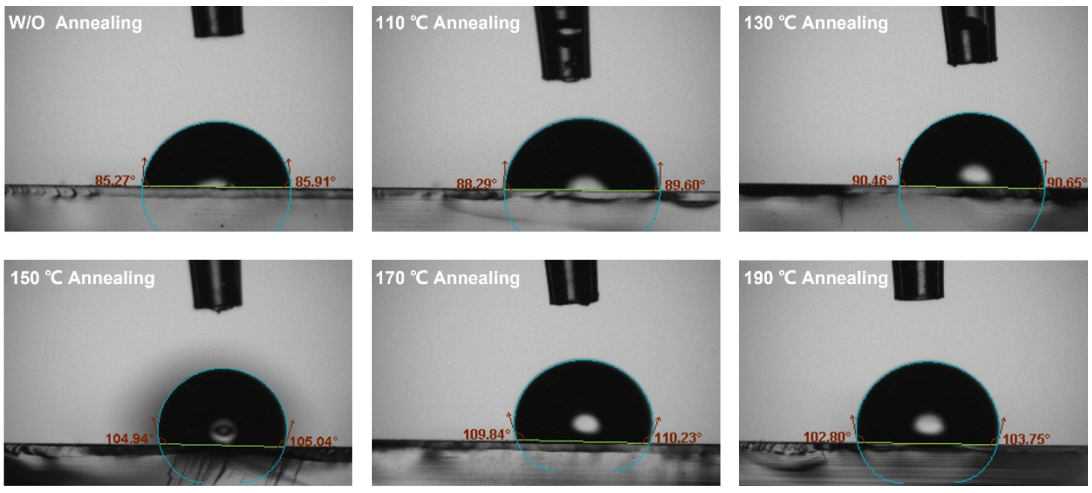


**Figure S3**. Contact angles of perovskite films W/O and with different annealing temperatures.

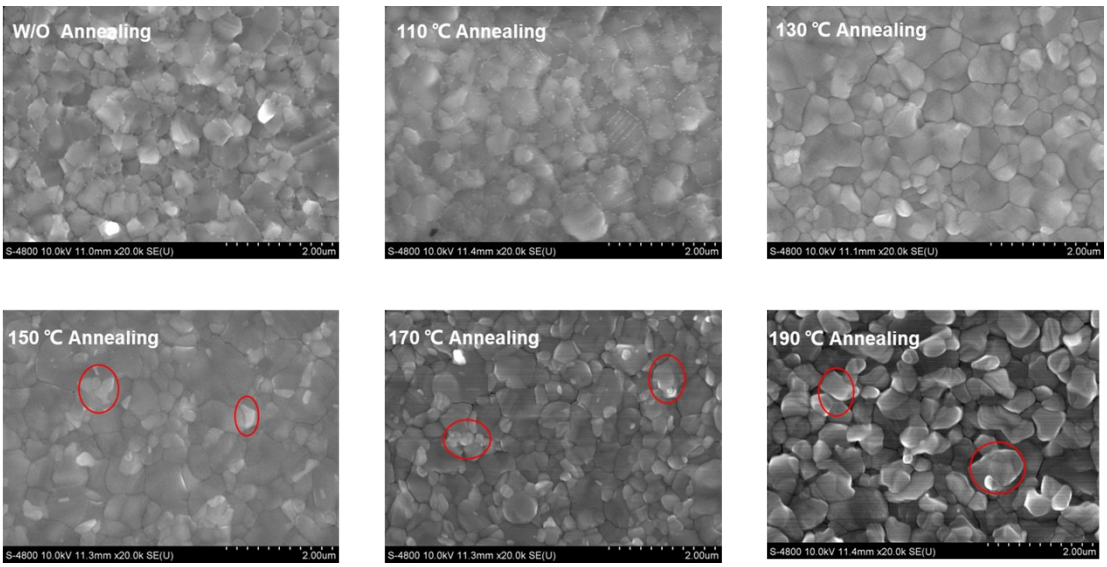


**Figure S4**. Top-view SEM images of perovskite films W/O and with different annealing temperatures.

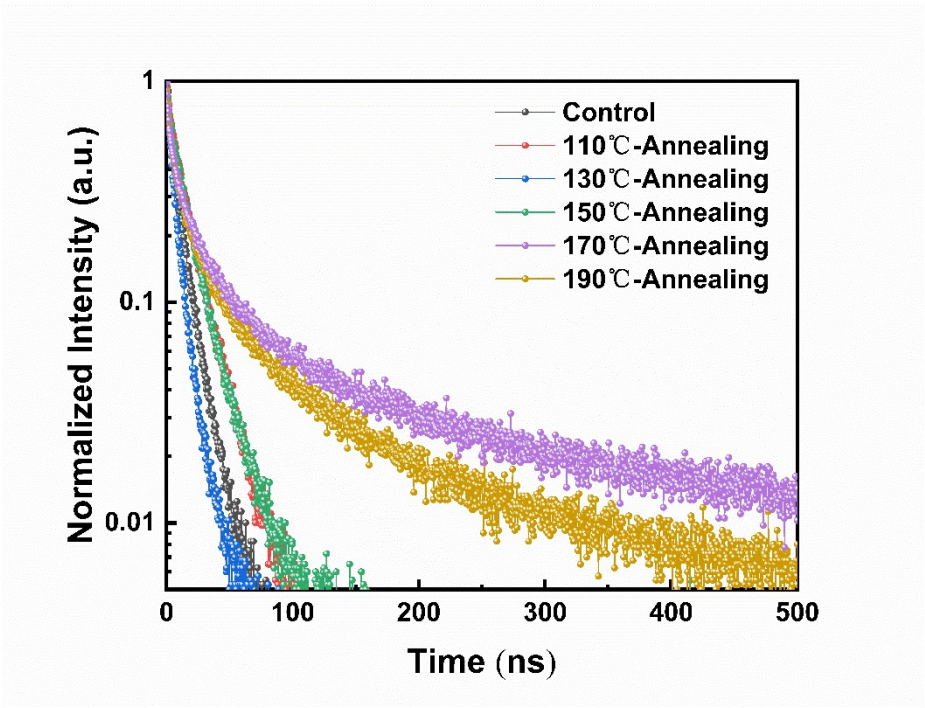


**Figure S5**. TRPL spectra of perovskite films W/O and with different annealing temperatures.

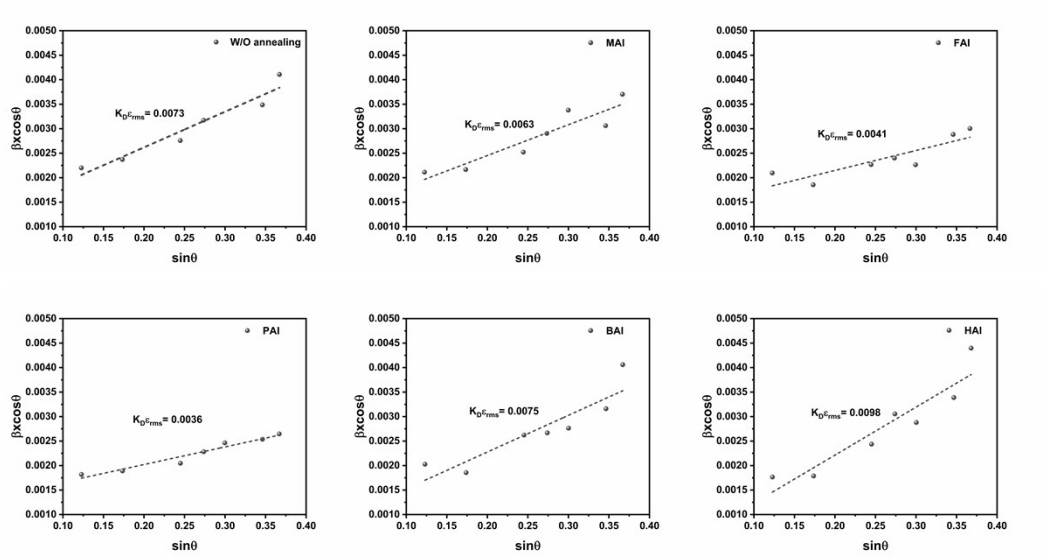


**Figure S6**. Williamson−Hall plots of perovskite films W/O and with Vapor-annealing of different organic ammonium salts.

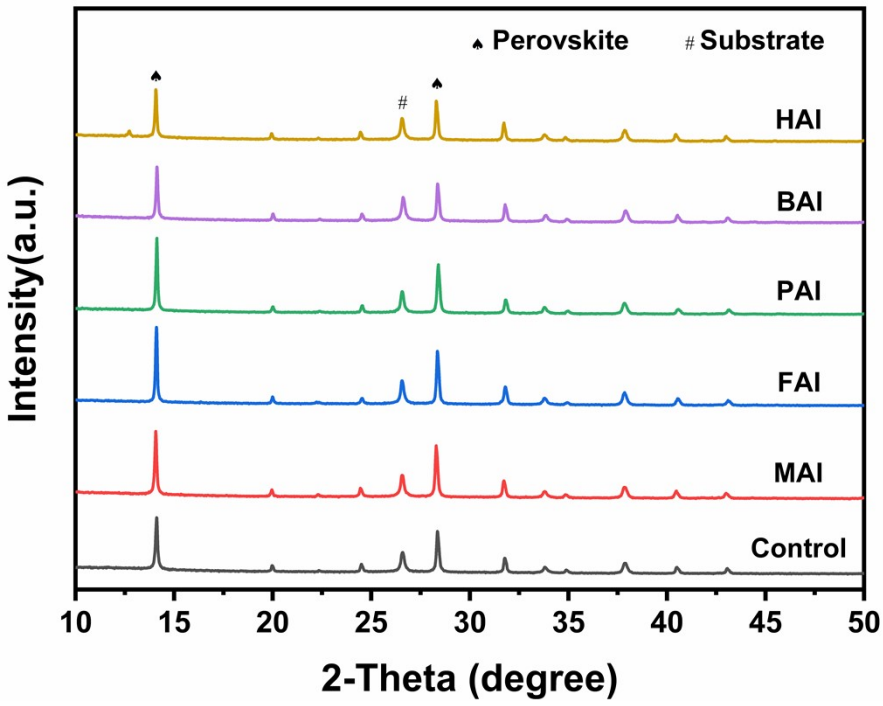


**Figure S7.** XRD patterns of the perovskite thin films W/O annealing and with different vapor annealing.

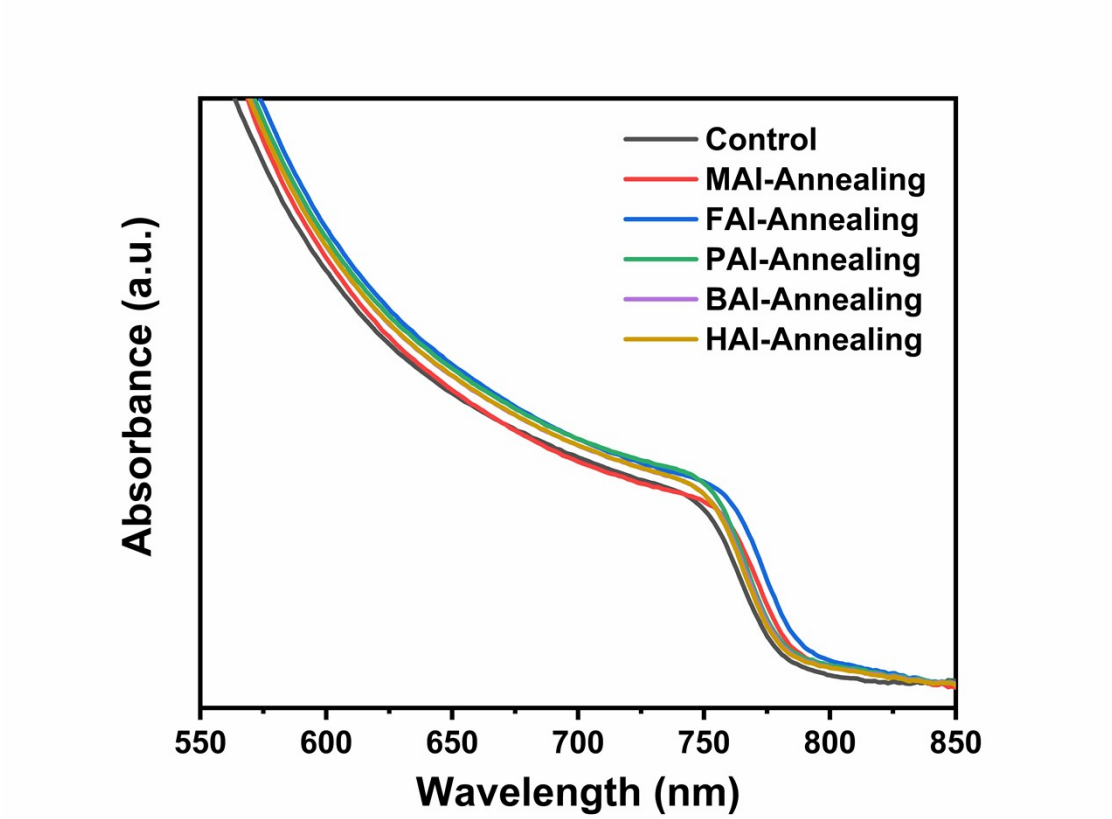


**Figure S8**. UV-vis absorption plots of the perovskite thin films W/O annealing and with different vapor annealing.

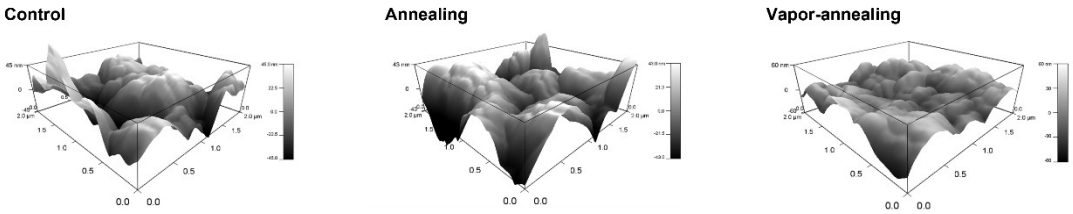


**Figure S9.** The AFM 3D topography images of perovskite films with Control, annealing and vapor annealing.

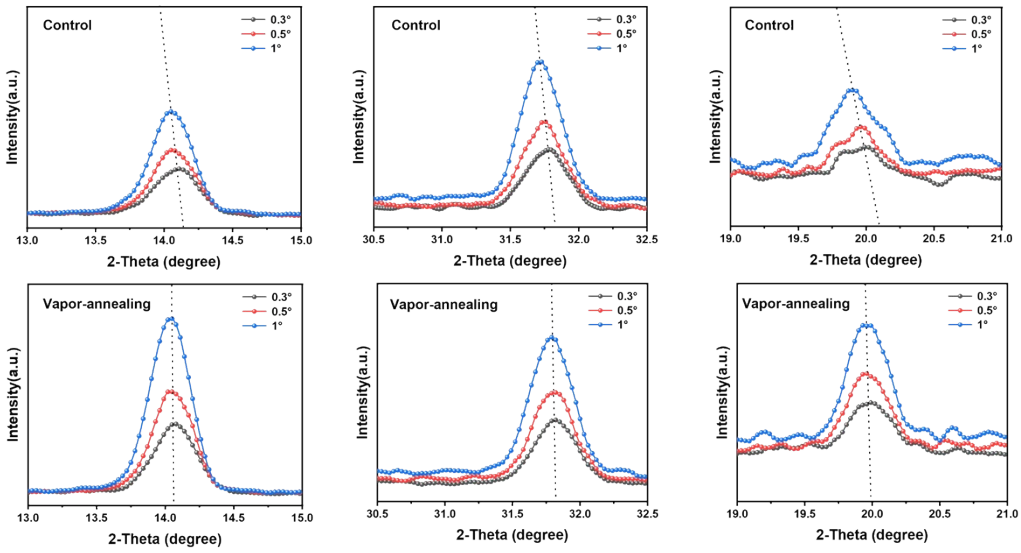


**Figure S10.** Different grazing incidence angles GIXRD patterns of the perovskite thin films W/O annealing and with vapor annealing.

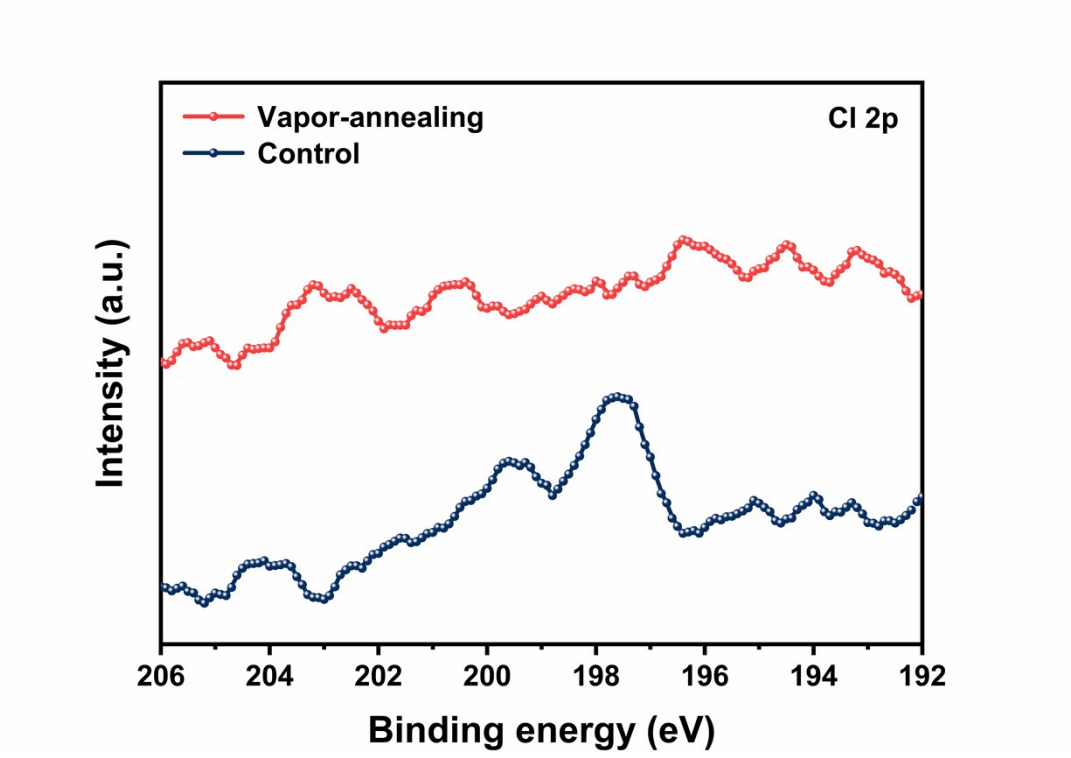


**Figure S11.** XPS spectra of the Cl 2p signal in the perovskite thin film W/O annealing and with vapor annealing.

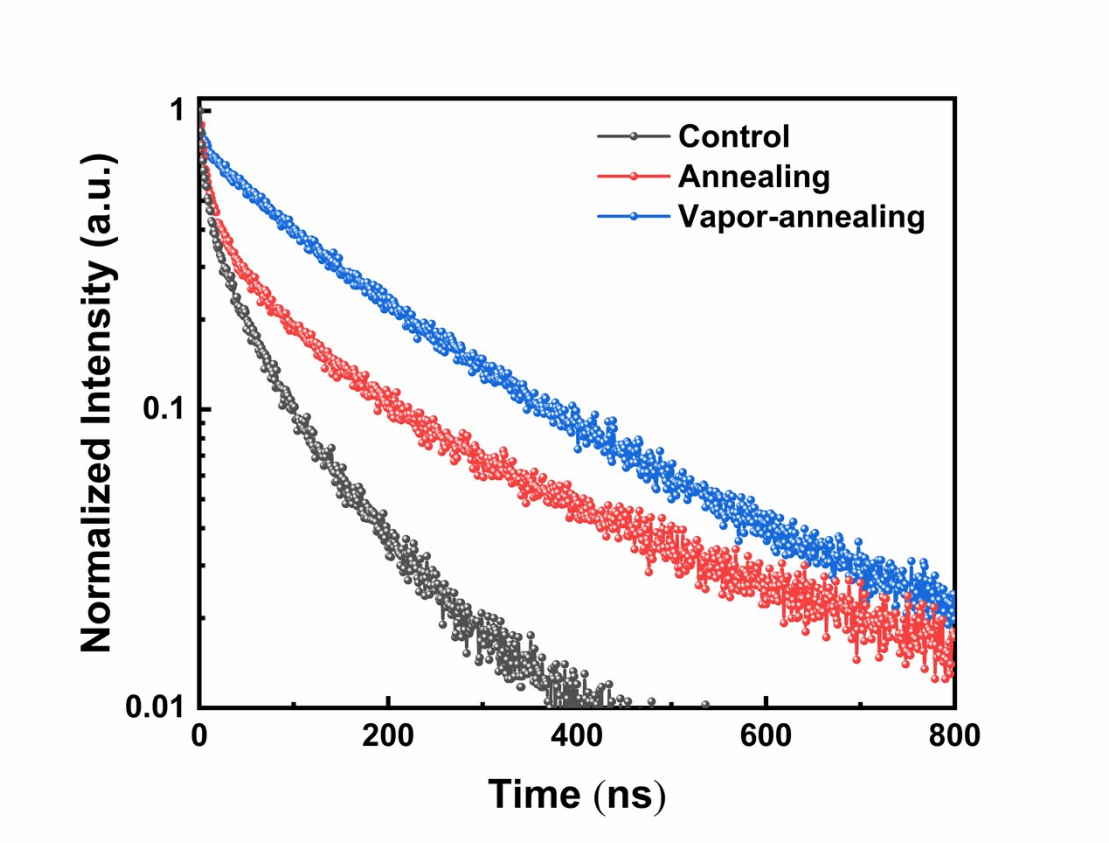


**Figure S12.** TRPL spectra of perovskite films W/O annealing, with annealing and with vapor annealing.

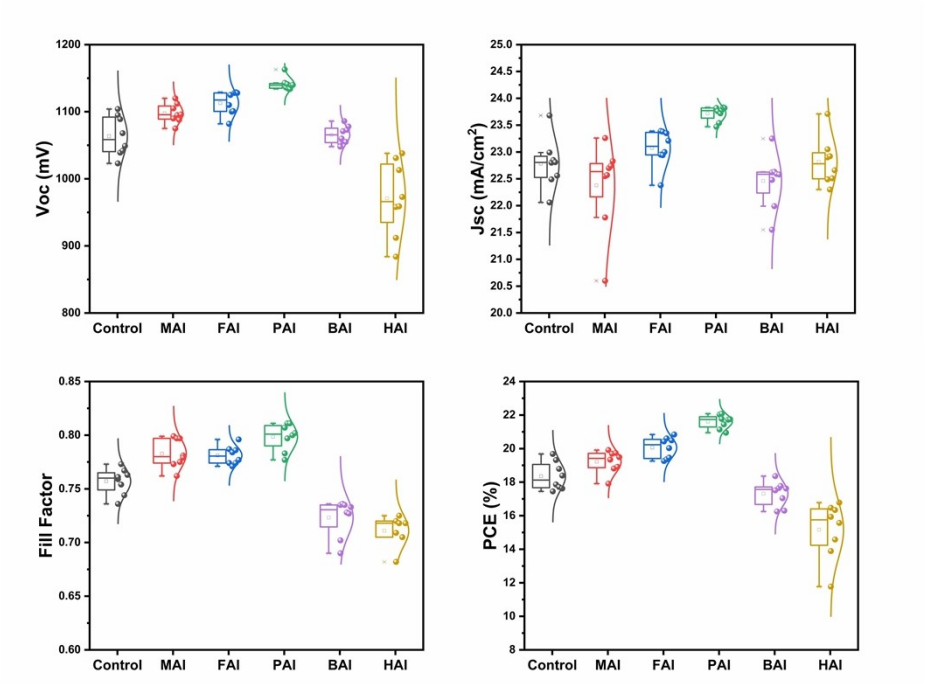


**Figure S13.** Statistical distribution diagram of the Voc, Jsc, FF, PCE of PSCs fabricated

by annealing in different ammonium salt vapors.

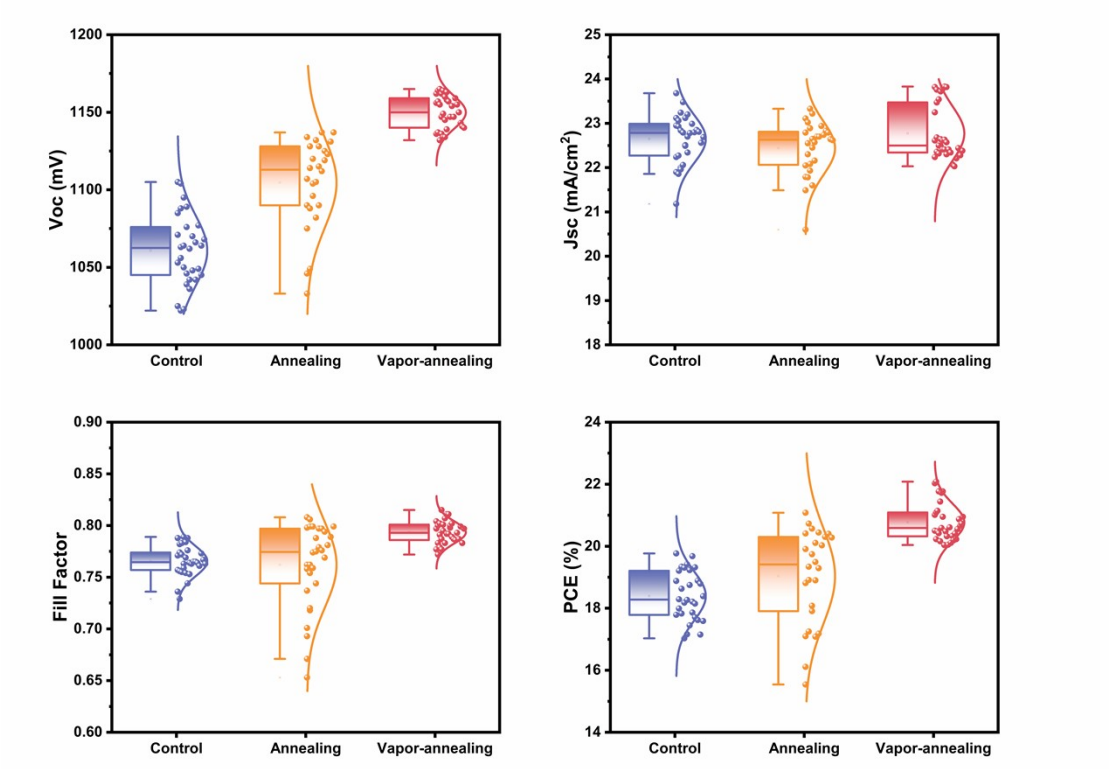


**Figure S14.** Statistical distribution diagram of the Voc, Jsc, FF, PCE of PSCs fabricated by Control, annealing and vapor annealing.

**Table S1**. Biexponential fitted TRPL parameters of the Control, Annealing and Vapor-annealing

| Samples | $A_1$ | $\tau_1$ (ns) | $A_2$ | $\tau_2$ (ns) | $\tau_{avg}$ (ns) |
|---|---|---|---|---|---|
| Control | 0.374 | 13.48 | 0.180 | 125.83 | 105.31 |
| Annealing | 0.337 | 26.07 | 0.290 | 174.8 | 152.83 |
| Vapor-annealing | 0.458 | 120.72 | 0.268 | 290.80 | 220.21 |

**Table S2** EIS Fitting parameters of solar cells based on Control and Vapor-annealing modified devices. The series resistance ($R_s$) and charge composite resistance ($R_{rec}$) can be obtained by data fitting of equivalent circuit diagram of PSCs by EC-Lab software.

| Sample | $R_s$ (Ω) | $R_{rec}$ (Ω) |
|---|---|---|
| Control | 9.544 | 20075.9 |
| Vapor-annealing | 9.012 | 41646.6 |